

Fig. 9. The variations of the isotropic thermal parameter of the S atom and its mean interatomic distance with two adjacent Ti and four adjacent Sr atoms as functions of  $t$  ( $= -0.57227x_3 + x_4$ ).

*Acta Cryst.* (1993). **B49**, 936–941

## Structure and Electrical Resistivity of the Heavy Fermion Compound CeCu<sub>5</sub>Au

BY M. RUCK

*Institut für Anorganische Chemie der Universität Karlsruhe, D-76128 Karlsruhe, Germany*

AND G. PORTISCH, H. G. SCHLAGER, M. SIECK AND H. V. LÖHNEYSSEN

*Physikalisches Institut der Universität Karlsruhe, D-76128 Karlsruhe, Germany*

(Received 14 April 1993; accepted 24 May 1993)

### Abstract

The crystal structure of CeCu<sub>5</sub>Au determined at room temperature is orthorhombic with space group *Pnma* (No. 62). The lattice constants are  $a = 8.2455(4)$ ,  $b = 5.0866(3)$  and  $c = 10.3659(5)$  Å with  $V = 434.76(7)$  Å<sup>3</sup> and four formula units per unit cell. Four-circle diffraction shows that CeCu<sub>5</sub>Au is an ordered intermetallic phase, isomorphous with CeCu<sub>6</sub>, with the Au atoms exclusively occupying the Cu(2) positions of the CeCu<sub>6</sub> structure. Measurements of the electrical resistivity of CeCu<sub>5</sub>Au at low temperatures yield a residual resistivity smaller than that of single crystals of CeCu<sub>5.5</sub>Au<sub>0.5</sub> by a factor of four, in line with the fact that CeCu<sub>5</sub>Au is a stoichiometric compound. The temperature dependence of the resistivity indicates magnetic ordering as found previously for CeCu<sub>6-x</sub>Au<sub>x</sub> with  $0.1 < x < 1$ .

### Introduction

The intermetallic compound CeCu<sub>6</sub>, a heavy fermion system (Grewe & Steglich, 1991) with an extraordinarily high linear contribution to the specific heat  $C$  [ $\gamma = C/T$  ( $T \rightarrow 0$ ) = 1.67 J mol<sup>-1</sup> K<sup>-2</sup> (Amato, Jaccard, Flouquet *et al.*, 1987)], is one of the few examples of these systems that neither show long-range magnetic order nor become superconducting down to the lowest measuring temperatures (10 mK in this case). On the other hand, short-range magnetic intersite correlations discovered by inelastic neutron scattering (Aeppli *et al.*, 1986; Rossat-Mignod *et al.*, 1988) and confirmed through the observation of a metamagnetic-like transition in magnetization measurements (Schröder, Schlager & Löhneysen, 1992) indicate the proximity of CeCu<sub>6</sub> to magnetic order. Indeed, substitution of Cu by Au leads

In this study, the crystal structure of the incommensurate composite crystal Sr<sub>1.145</sub>TiS<sub>3</sub> was successfully analysed in a four-dimensional formalism using the Rietveld analysis process based on the powder X-ray diffraction data, because satellite intensities up to the sixth order were strong enough to be detected by the powder method as described above.

The authors wish to express appreciation to Mr Y. Kitami for help in electron-diffraction experiments.

### References

- HAHN, H. & MUTSCHKE, U. (1956). *Z. Anorg. Allg. Chem.* **288**, 269–278.  
 JANNER, A. & JANSSEN, T. (1980). *Acta Cryst.* **A36**, 408–415.  
 KATO, K. & ONODA, M. (1991a). *Acta Cryst.* **A47**, 55–56.  
 KATO, K. & ONODA, M. (1991b). *Acta Cryst.* **A47**, 448–449.  
 KATO, K. & ONODA, M. (1992). *Acta Cryst.* **A48**, 73–76.  
 SAEKI, M. & ONODA, M. (1993). *J. Solid State Chem.* **102**, 100–105.  
 UKEI, K., YAMAMOTO, A., WATANABE, Y., SHISHIDO, T. & FUKUDA, T. (1993). *Acta Cryst.* **B49**, 67–72.  
 YAMAMOTO, A. (1992). *Acta Cryst.* **A48**, 476–483.  
 YAMAMOTO, A., TAKAYAMA-MUROMACHI, E., IZUMI, F., ISHIGAKI, T. & ASANO, H. (1992). *Physica C*, **201**, 137–144.

to an instability of the coherent Kondo ground state with respect to antiferromagnetic order *via* the RKKY interaction as proven by elastic neutron scattering investigations of  $\text{CeCu}_{5.5}\text{Au}_{0.5}$ , yielding an incommensurate antiferromagnetic structure (Chattopadhyay, Löhneysen, Trappmann & Loewenhaupt, 1990). The occurrence of magnetic order can be explained in terms of the Doniach picture (Doniach, 1977) by the weakening of the antiferromagnetic exchange coupling  $J$  between the conduction electrons and the  $4f$  electrons of the Ce atoms as a result of the lattice expansion caused by the larger Au atomic radius (Trappmann, 1991; Schlager, Schröder, Welsch & Löhneysen, 1993).

Besides the lattice expansion, a major effect of alloying with Au is the introduction of disorder into the regular Kondo lattice of pure  $\text{CeCu}_6$ . As a consequence, the coherence of the Kondo ions, which is seen in the steep decrease of the electrical resistivity  $\rho$  of  $\text{CeCu}_6$  towards low temperatures, is weakened as was shown by resistivity measurements on single crystals of  $\text{CeCu}_{5.5}\text{Au}_{0.5}$  (Schlager *et al.*, 1993). The intensity of the reflections of powder X-ray diffraction patterns of various  $\text{CeCu}_{6-x}\text{Au}_x$  samples lead to the suggestion that the Au atoms are not distributed randomly among the different Cu sites in the crystal lattice of  $\text{CeCu}_6$  (Mock, Schröder, Sereni, Sieck & Löhneysen, 1993) but substitute exclusively Cu atoms at the Cu(2) site of the orthorhombic structure (space group *Pnma*; Cromer, Larson & Roof, 1960). The main purpose of the X-ray investigations and the resistivity measurements on  $\text{CeCu}_5\text{Au}$  single crystals which we present in this paper is to show that this is indeed the case and that the full periodicity of the lattice is recovered in  $\text{CeCu}_5\text{Au}$ .

#### Crystal growth and characterization

The  $\text{CeCu}_5\text{Au}$  crystal was pulled from a tungsten crucible by the Czochralski method using 5 N Cu (Alfa, Karlsruhe), 5 N Ce (Ames Laboratory, Iowa State University) and 4 N Au (Alfa, Karlsruhe) as starting materials. To avoid contamination with cerium oxides and changes of the stoichiometry of the melt due to evaporation of the volatile components, the growth process was performed in a high-purity argon atmosphere under a pressure of  $3.5 \times 10^5$  Pa. Because of the lack of a suitable seed, the necking-down technique was applied so that the growth interface was dominated by one crystallite. A cylindrical crystal of about 6 mm in diameter was pulled out of the melt with a speed of  $18 \text{ mm h}^{-1}$  and a rotation frequency of  $3 \text{ min}^{-1}$ .

X-ray diffraction ( $\theta$ - $2\theta$  scans, Cu  $K\alpha$  radiation) on powder ground from small portions of the crystal showed the structure to be orthorhombic at room temperature with lattice constants  $a = 8.250$ ,  $b = 5.084$  and  $c = 10.36$  Å. No reflections of cerium oxides or other phases could be detected.

The Au concentration, measured by atomic absorption spectroscopy (AAS) on small samples taken from different locations along the growth direction of the crystal, did not vary significantly and agreed within 1% with the primary concentration of the melt, thus showing that the distribution coefficient of Au in this system does not deviate much from 1. The crystal was also checked by AAS for possible contamination. The concentration of Fe was found to be 5 p.p.m., a value which is an order of magnitude less than that of  $\text{CeCu}_6$  single crystals which had been grown previously by the same technique (Onuki *et al.*, 1987). Unfortunately, the detection limit of the AAS for W is about 500 p.p.m., so that contamination from the crucible material can only be ruled out on this scale. Onuki *et al.* found no W contamination in their  $\text{CeCu}_6$  crystals within the detection limit of 40 p.p.m. (Onuki *et al.*, 1985). Therefore W impurities are assumed to be negligible in our crystals, also.

Laue pictures with a broad X-ray spot indicated that the resulting crystal consisted of several large crystallites with small-angle grain boundaries ( $<2^\circ$ ). A single crystal of dimensions  $2 \times 3 \times 4$  mm, the faces oriented perpendicular to the three orthorhombic axes, could be cut from the sample by spark erosion. To avoid contamination, this technique was also used for dividing this single crystal into smaller samples for measurements of specific heat, magnetization and electrical resistivity. The samples for the X-ray investigations were chosen from a ground portion of the original crystal.

#### X-ray single-crystal investigations

Precession photographs taken at room temperature showed the crystals to be orthorhombic. The reflection conditions (reflections  $0kl$  were observed only with  $k + l = 2n$  and reflections  $hk0$  only with  $h = 2n$ ) indicated the space group to be *Pn2<sub>1</sub>a* or *Pnma*; the structure refinement showed the latter to be correct. Cell dimensions were determined by the least-squares method from accurately measured Laue angles of 168 single-crystal reflections including correction for displacement caused by absorption effects (Nelson & Riley, 1945). The lattice constants and space group permitted the assumption that the structure of  $\text{CeCu}_5\text{Au}$  is isomorphous to that of  $\text{CeCu}_6$  (Cromer *et al.*, 1960).

An irregularly formed fragment of the large crystal with approximate dimensions  $0.25 \times 0.25 \times 0.35$  mm was used for intensity collection. 5911 intensities were recorded at room temperature on an automated four-circle diffractometer (AED-2, Siemens/Stoe) with Mo  $K\alpha$  radiation ( $\lambda = 0.71073$  Å) monochromated by graphite up to  $2\theta = 70^\circ$ , employing the  $\omega$ - $\theta$  scan technique. The scan rate varied between 3 and  $0.5^\circ \text{ min}^{-1}$  depending on the ratio  $I/\sigma(I)$ . The intensities were corrected for background, Lorentz and polarization

factors. Because of the high linear absorption coefficient  $\mu(\text{Mo } K\alpha) = 653 \text{ cm}^{-1}$ , special care was devoted to the numerical absorption correction. Based upon eight suitable  $\psi$  profiles a preliminary description of the crystal shape including 16 faces was optimized using the program *HABITUS* (Bärnighausen & Herrendorf, 1992). The transmission factors ranged between 0.001 and 0.020.

207 single intensities which deviated significantly from the mean of the other members of a corresponding set of equivalent reflections were disregarded before averaging. 1029 unique reflections were employed for full-matrix least-squares structure refinement (program *SHELX76*; Sheldrick, 1976) applying no further acceptance criterion. Atomic scattering factors for neutral atoms and real and imaginary parts of the anomalous dispersion were taken from *International Tables for X-ray Crystallography* (1974, Vol. IV).

The atomic coordinates of CeCu<sub>6</sub> were taken as the initial parameters. In this structure the Cu-atom position with the highest coordination number CN = 14 and the largest value for the mean interatomic distance in the coordination sphere with respect to CN = 12, *i.e.* Cu(2) in CeCu<sub>6</sub>, was replaced by the Au atom. This proved to be the correct position. For testing purposes the occupancy of the Au position was allowed to vary. It refined to 0.991 with an estimated standard deviation of 0.005 and thus it can be assumed that within the experimental accuracy this position is exclusively occupied by Au.

An empirical isotropic extinction parameter  $x = 9.3 \times 10^{-8}$  was applied, where the calculated structure factors  $F_c$  are multiplied by  $(1 - xF_c^2/\sin\theta)$ . The refinement involving anisotropic displacement factors (41 parameters) converged well leading to final values of  $R = \sum ||F_o| - |F_c|| / \sum |F_o| = 0.028$  and  $wR = [\sum w(|F_o| - |F_c|)^2 / \sum wF_o^2]^{1/2} = 0.023$ . The weighting scheme was  $w = \sigma(F_o)^{-2}$  with  $\sigma(F_o)$  being based on the mean of the counting statistics as well as on the standard deviation of the averaging procedure. A final difference Fourier map showed the residual electron density to vary between 2.4 and  $-2.8 \text{ e } \text{Å}^{-3}$  with maxima lying in the vicinity of atomic positions. The final structural parameters for CeCu<sub>5</sub>Au are listed in Table 1.\* For the calculation of interatomic distances given in Table 2 the program *ORFFEII* (Busing, Martin & Levy, 1967) was used. The crystal structure drawings were prepared with the program *ORTEPII* (Johnson, 1976).

CeCu<sub>5</sub>Au is isomorphous to CeCu<sub>6</sub> at room temperature. It is the first ternary compound that is known to adopt this structure type while there are another eight binary examples (Villars, Matthis & Hulliger, 1989).

\* Lists of structure factors and anisotropic thermal parameters have been deposited with the British Library Document Supply Centre as Supplementary Publication No. 71239 (14 pp.). Copies may be obtained through The Technical Editor, International Union of Crystallography, 5 Abbey Square, Chester CH1 2HU, England. [CIF reference: SE0121]

Table 1. *Atomic parameters for CeCu<sub>5</sub>Au*

The constant  $B$  ( $\text{Å}^2$ ) of the Debye-Waller factor  $\exp(-B\sin^2\theta/\lambda^2)$  was calculated from the coefficients  $U_{ij}$  of the tensor of the anisotropic displacement factor (Hamilton, 1959). Standard deviations are given in parentheses.

		x	y	z	B
Ce	4(c)	0.26078 (4)	$\frac{1}{2}$	0.43593 (3)	0.98 (2)
Cu(1)	8(d)	0.43493 (7)	0.0013 (1)	0.18791 (4)	1.00 (2)
Cu(2)	4(c)	-0.09178 (9)	$\frac{1}{2}$	-0.48395 (6)	1.11 (3)
Cu(3)	4(c)	-0.18475 (9)	$\frac{1}{2}$	-0.25071 (6)	1.11 (3)
Cu(4)	4(c)	-0.44400 (9)	$\frac{1}{2}$	-0.39553 (6)	1.29 (3)
Au	4(c)	0.14216 (3)	$\frac{1}{2}$	0.13897 (2)	1.08 (1)

Table 2. *Interatomic distances for CeCu<sub>5</sub>Au* ( $\text{Å}$ )

Standard deviations are given in parentheses

Ce—Cu(2)	2.9425 (4) 2 ×	Cu(1)—Cu(2)	2.4737 (7) 1 ×
Ce—Cu(4)	2.9876 (4) 2 ×	Cu(1)—Cu(4)	2.5043 (7) 1 ×
Ce—Cu(4)	2.9962 (8) 1 ×	Cu(1)—Cu(3)	2.5063 (9) 1 ×
Ce—Cu(2)	3.0234 (8) 1 ×	Cu(1)—Cu(3)	2.5125 (8) 1 ×
Ce—Cu(1)	3.2051 (6) 2 ×	Cu(1)—Cu(1)	2.531 (1) 1 ×
Ce—Au	3.2299 (4) 1 ×	Cu(1)—Cu(2)	2.5455 (8) 1 ×
Ce—Cu(1)	3.2354 (6) 2 ×	Cu(1)—Cu(1)	2.556 (1) 1 ×
Ce—Au	3.2390 (4) 1 ×	Cu(1)—Au	2.7724 (6) 1 ×
Ce—Cu(3)	3.2477 (5) 2 ×	Cu(1)—Au	2.7823 (6) 1 ×
Ce—Cu(3)	3.2938 (7) 1 ×	Cu(1)—Ce	3.2051 (6) 1 ×
Ce—Cu(1)	3.3257 (6) 2 ×	Cu(1)—Ce	3.2353 (6) 1 ×
Ce—Au	3.3968 (3) 2 ×	Cu(1)—Ce	3.3257 (6) 1 ×
Cu(2)—Cu(1)	2.4737 (7) 2 ×	Cu(3)—Cu(4)	2.498 (1) 1 ×
Cu(2)—Cu(3)	2.5364 (9) 1 ×	Cu(3)—Cu(1)	2.5063 (9) 2 ×
Cu(2)—Cu(1)	2.5455 (8) 2 ×	Cu(3)—Cu(1)	2.5125 (8) 2 ×
Cu(2)—Au	2.7193 (8) 1 ×	Cu(3)—Cu(2)	2.5364 (9) 1 ×
Cu(2)—Ce	2.9425 (4) 2 ×	Cu(3)—Cu(4)	2.612 (1) 1 ×
Cu(2)—Cu(2)	2.9783 (8) 2 ×	Cu(3)—Au	2.8166 (3) 2 ×
Cu(2)—Ce	3.0234 (8) 1 ×	Cu(3)—Ce	3.2477 (5) 2 ×
Cu(2)—Cu(4)	3.045 (1) 1 ×	Cu(3)—Ce	3.2938 (7) 1 ×
Cu(4)—Cu(3)	2.498 (1) 1 ×	Au—Cu(4)	2.6214 (7) 1 ×
Cu(4)—Cu(1)	2.5043 (7) 2 ×	Au—Cu(2)	2.7193 (8) 1 ×
Cu(4)—Cu(3)	2.612 (1) 1 ×	Au—Cu(1)	2.7724 (6) 2 ×
Cu(4)—Au	2.6214 (7) 1 ×	Au—Cu(1)	2.7823 (6) 2 ×
Cu(4)—Ce	2.9876 (5) 2 ×	Au—Cu(3)	2.8166 (3) 2 ×
Cu(4)—Ce	2.9962 (8) 1 ×	Au—Cu(4)	3.0440 (5) 2 ×
Cu(4)—Au	3.0440 (5) 2 ×	Au—Ce	3.2299 (4) 1 ×
Cu(4)—Cu(2)	3.045 (1) 1 ×	Au—Ce	3.2390 (4) 1 ×
Cu(4)—Cu(4)	3.4657 (9) 2 ×	Au—Ce	3.3968 (3) 2 ×

With the Au atom occupying one discrete crystallographic position, CeCu<sub>5</sub>Au is to be regarded as an ordered intermetallic phase. Thus, it can be argued that for all compositions CeCu<sub>6-x</sub>Au<sub>x</sub> with  $x < 1$  only this particular position is statistically occupied by Cu and Au. This assumption is supported by powder diffraction data of polycrystalline samples with intermediate Au content (Mock *et al.*, 1993).

The Ce atom has the high and rather unusual coordination number of CN = 19. Five Cu atoms and one Au atom form an approximately regular hexagon around it (Fig. 1). The other neighbouring atoms are arranged in a pentagonal pyramid below and a hexagonal pyramid above this ring. The polyhedron shows six rhombic and 22 trigonal faces. Following Daams, Villars & Van Vucht (1988) it can be described with the symbol  $6^4.16^2.23^5.03^3.216.0$ .\*

\* These symbols are based on the number of triangles and squares that join in the different vertices. The symbols indicate the number of equivalent corners with the number of triangular and square faces (in this sequence) given as superscripts.

The coordination polyhedra of all other atoms (Fig. 1) show a pseudo-threefold axis neglecting the distinction between Cu and Au. Although Cu(1) and Cu(3) do not have the same site symmetry their coordination polyhedra are very similar and may be described as distorted icosahedra (symbol  $12^{5.0}$ ) with two of the triangular faces being almost coplanar. This similarity is also expressed by nearly equal displacement parameters and mean interatomic distances inside the coordination polyhedra.

The arrangement of the 12 nearest neighbours around Cu(2) can be derived from an anticuboctahedron by a  $30^\circ$  rotation of the equatorial hexagon about the threefold axis. The polyhedron has 20 triangular faces and can be described by the symbol  $6^{5.0}3^6.03^4.0$ .

According to the maximum-gap method (Brunner & Schwarzenbach, 1971) the coordination number of Cu(4) is CN = 13. The connection between the 16 triangular and three rhombic faces of the polyhedron is given by the symbol  $6^{5.0}3^4.13^2.21^0.3$ . However, it has to be mentioned that two of the neighbouring atoms are considerably more distant from the central Cu(4) atom. Compared with the values for the other three Cu atoms the mean of the interatomic distances towards Cu(4) is about

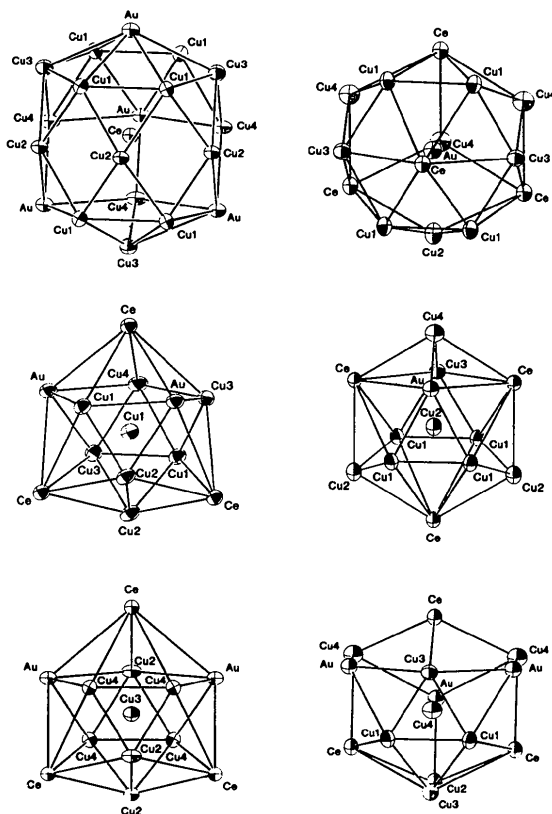


Fig. 1. Coordination polyhedra in the crystal structure of  $\text{CeCu}_5\text{Au}$ . The surfaces of the displacement ellipsoids are drawn at the 90% probability level.

Table 3. Mean interatomic distances,  $\overline{[n]d}$  (Å), towards the central atoms in the coordination polyhedra for  $\text{CeCu}_5\text{Au}$  and  $\text{CeCu}_6$

The coordination number is given by the index  $[n]$ .  $\Delta\overline{[n]d}$  indicates the difference of  $\overline{[n]d}$  for corresponding sites in  $\text{CeCu}_5\text{Au}$  and  $\text{CeCu}_6$ . [Note that Cu(2) in  $\text{CeCu}_5\text{Au}$  corresponds to Cu(5) in  $\text{CeCu}_6$ .]

$\text{CeCu}_5\text{Au}$		$\text{CeCu}_6$		$\Delta\overline{[n]d}$
Ce	$\overline{[12]d} = 3.182$	Ce	$\overline{[12]d} = 3.146$	0.036
Cu(1)	$\overline{[12]d} = 2.746$	Cu(1)	$\overline{[12]d} = 2.721$	0.025
Cu(2)	$\overline{[12]d} = 2.767$	Cu(5)	$\overline{[12]d} = 2.748$	0.019
Cu(3)	$\overline{[12]d} = 2.759$	Cu(3)	$\overline{[12]d} = 2.734$	0.025
Cu(4)	$\overline{[11]d} = 2.804$	Cu(4)	$\overline{[11]d} = 2.779$	0.025
	$\overline{[13]d} = 2.906$		$\overline{[13]d} = 2.872$	0.034
Au	$\overline{[12]d} = 2.887$	Cu(2)	$\overline{[12]d} = 2.840$	0.047
	$\overline{[14]d} = 2.960$		$\overline{[14]d} = 2.918$	0.042

0.1 Å larger (Table 3). Hence the significantly enlarged displacement parameter of Cu(4) can be understood.

Similar to the situation around Cu(4), two of the interatomic distances between Au and the 14 atoms in its coordination sphere are significantly longer. The polyhedron has been described by Cromer *et al.* (1960). It can be visualized as a tetrahedron formed by four Ce atoms with a triangle of three Cu atoms above three faces of this tetrahedron. The fourth face is capped by a single Cu atom. The symbol  $6^{5.0}3^3.23^3.11^6.01^0.3$  gives the connection of the three rhombic and 18 triangular faces of this polyhedron.

In comparison to  $\text{CeCu}_6$ , the lattice parameters  $a = 8.2455(4)$  and  $c = 10.3659(5)$  Å of  $\text{CeCu}_5\text{Au}$  are increased by 1.6 and 2.0%, respectively, while  $b = 5.0866(3)$  Å is slightly decreased by 0.4%. These lattice parameters agree within 0.1% with an extrapolation of powder diffraction data of  $\text{CeCu}_{6-x}\text{Au}_x$  with various compositions in the range  $0 \leq x \leq 0.9$  (Trappmann, 1991; Schlager *et al.*, 1993) and also with the powder diffraction data for the same sample mentioned above. The difference of  $14.2 \text{ \AA}^3$  between the volumes of the unit cells is smaller than the expected value of  $20.4 \text{ \AA}^3$  based on the volume increments for neutral atoms listed by Biltz (1934). The atomic radii found in elemental Cu and Au (CN = 12) are  $^{[12]}r(\text{Cu}) = 1.28$  and  $^{[12]}r(\text{Au}) = 1.44$  Å. Thus, regarding atoms as hard spheres the replacement of four Cu atoms per unit cell by Au atoms should lead to an increase in the unit-cell volume of about  $14.9 \text{ \AA}^3$  which is in good agreement with the observed value. However, the additional volume of  $14.2 \text{ \AA}^3$  cannot be assigned exclusively to the spatial requirement of the Au atom because the coordination spheres of all atoms are affected by a common dilatation of interatomic distances (*cf.* Table 3).

This can be rationalized by the fact that the Cu atom (in  $\text{CeCu}_6$ ) being replaced by Au (in  $\text{CeCu}_5\text{Au}$ ) is the one with the highest coordination number, the largest value for the mean interatomic distance in the coordination sphere (with respect to CN = 12) and a large displacement parameter. Therefore the Cu atom may be assumed to fill up the available space insufficiently while a larger atom like Au is more suited for that site. In

consequence it is expected that further substitution of Cu by Au ( $x > 1$ ) would occur preferentially at a site offering similar conditions, *i.e.* Cu(4).

For further work, it would be interesting to see if CeCu<sub>5</sub>Au remains orthorhombic upon cooling to low temperature. It is well known that CeCu<sub>6</sub> undergoes a slight monoclinic distortion (with a deviation of about 1.5° from a right angle) around 200 K (Vrtis, Jorgensen & Hinks, 1986; Gratz *et al.*, 1987).

### Electrical resistivity

The electrical resistivity was measured with a standard four-probe low frequency a.c. method in a dilution refrigerator in the temperature range from 0.01 to 6 K. The sample was mounted in a special clamp with W blades having a fixed distance as voltage probes. The temperature dependence of the electrical resistivity  $\rho(T)$  of CeCu<sub>6-x</sub>Au<sub>x</sub> for  $x = 0, 0.5$  and 1 along the crystallographic  $b$  axis is shown in Fig. 2. For CeCu<sub>6</sub> the resistivity  $\rho(T)$  displays a broad maximum around 10 K (beyond the  $T$  range of Fig. 2), a rapid decrease and a  $T^2$  law at low temperatures, indicating the transition to coherent scattering in a periodic Kondo lattice (Onuki *et al.*, 1987; Amato, Jaccard, Walker, Sierro & Flouquet, 1987).

Alloying with Au has two main effects which can both be observed in the resistivity:

(1) The translational symmetry is disturbed which affects the Bloch states of the conduction electrons leading to an increase of the residual electrical resistivity  $\rho_0$  (Löhneysen, Schröder, Trappmann & Welsch, 1992).

(2) For  $x > 0.1$  long-range antiferromagnetic order occurs, seen here as a maximum in  $\rho(T)$  of the

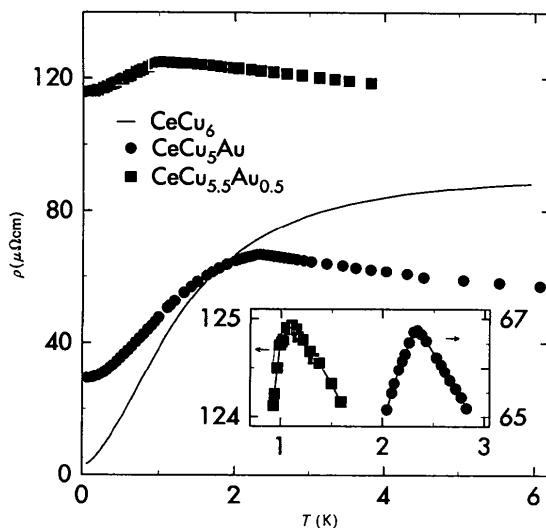


Fig. 2. Electrical resistivity  $\rho$  of CeCu<sub>6-x</sub>Au<sub>x</sub> single crystals versus temperature  $T$  measured with current direction parallel to  $b$ . Inset shows  $\rho(T)$  in the vicinity of the antiferromagnetic transition for  $x = 0.5$  and 1.

CeCu<sub>5.5</sub>Au<sub>0.5</sub> crystal at the Néel temperature  $T_N = 0.95$  K.

The non-stoichiometric CeCu<sub>5.5</sub>Au<sub>0.5</sub> shows the largest  $\rho_0$  (Schlager *et al.*, 1993), enhanced by a factor of 20 to 25 compared to CeCu<sub>6</sub>, while  $\rho_0$  of the stoichiometric CeCu<sub>5</sub>Au is reduced to ~25% of this maximum value. In CeCu<sub>5.5</sub>Au<sub>0.5</sub> half of the Cu(2) sites are statistically occupied by Au. Hence the alloy is the most disturbed of the three samples in the plot and is therefore expected to have the largest residual value of  $\rho_0$ . Since CeCu<sub>5</sub>Au is a stoichiometric compound with an undisturbed crystal symmetry,  $\rho_0$  should be much smaller than observed. Further investigations have to be carried out to clarify this point. The maximum of  $\rho(T)$  at  $T_N = 2.3$  K signals the antiferromagnetic phase transition.

In conclusion, we mention that  $T_N(x)$  exhibits a sharp maximum for  $x = 1$ , although the structure remains single-phase orthorhombic up to  $x \simeq 1.5$  (Mock *et al.*, 1993). This again points out the special role CeCu<sub>5</sub>Au, with just all the Cu(2) sites of CeCu<sub>6</sub> occupied by Au, plays in this substitution series. The thermodynamic and magnetic properties of CeCu<sub>5</sub>Au single crystals will be reported elsewhere (Löhneysen *et al.*, 1993).

We thank H. Bärnighausen for valuable discussions.

### References

- AEPPLI, G., YOSHIZAWA, H., ENDOH, Y., BUCHER, E., HUFNAGL, J., ONUKI, Y. & KOMATSUBARA, T. (1986). *Phys. Rev. Lett.* **57**(1), 122-125.
- AMATO, A., JACCARD, D., FLOUQUET, J., LAPIERRE, F., THOLENCE, J. L., FISHER, R. A., LACEY, S. E., OLSEN, J. A. & PHILLIPS, N. E. (1987). *J. Low Temp. Phys.* **68**(5/6), 371-397.
- AMATO, A., JACCARD, D., WALKER, E., SIERRO, J. & FLOUQUET, J. (1987). *J. Magn. Magn. Mater.* **63/64**, 300-302.
- BÄRNIGHAUSEN, H. & HERRENDORF, W. (1992). *HABITUS. Program for Crystal Shape Optimization by  $\psi$  Profiles*. Univ. of Karlsruhe, Germany.
- BILTZ, W. (1934). *Raumchemie der festen Stoffe*, pp. 238-239. Leipzig: Verlag Leopold Voss.
- BRUNNER, G. O. & SCHWARZENBACH, D. (1971). *Z. Kristallogr.* **133**, 127-133.
- BUSING, W. R., MARTIN, K. O. & LEVY, H. A. (1967). *ORFFELI*. Report ORNL-TM-306. Oak Ridge National Laboratory, Tennessee, USA.
- CHATTOPADHYAY, T., LÖHNEYSSEN, H. v., TRAPPMANN, T. & LOEWENHAUPT, M. (1990). *Z. Phys. B*, **80**, 159-160.
- CROMER, D. T., LARSON, A. C. & ROOF, R. B. (1960). *Acta Cryst.* **13**, 913-918.
- DAAMS, J., VILLARS, P. & VUCHT, J. VAN (1988). *Z. Kristallogr.* **185**, 714.
- DONIACH, S. (1977). *Physica B*, **91**, 231-234.
- GRATZ, E., BAUER, E., NOWOTNY, H., MUELLER, H., ZEMIRLI, S. & BARBARA, B. (1987). *J. Magn. Magn. Mater.* **63/64**, 312-314.
- GREWE, N. & STEGLICH, F. (1991). *Handbook on the Physics and Chemistry of Rare Earths*, Vol. 14, edited by K. A. Gschneidner Jr & L. Eyring, pp. 343-474. Amsterdam: Elsevier.
- HAMILTON, W. C. (1959). *Acta Cryst.* **12**, 609-610.
- JOHNSON, C. K. (1976). *ORTEPII*. Report ORNL-5138. Oak Ridge National Laboratory, Tennessee, USA.
- LÖHNEYSSEN, H. v., PASCHKE, C., PORTISCH, G., RUCK, M., SCHLAGER, H. G., SIECK, M. & SPECK, C. (1993). *Physica B*. In the press.
- LÖHNEYSSEN, H. v., SCHRÖDER, A., TRAPPMANN, T. & WELSCH, M. (1992). *J. Magn. Magn. Mater.* **108**, 45-46.

- MOCK, S., SCHRÖDER, A., SERENI, J., SIECK, M. & LÖHNEYSEN, H. v. (1993). In preparation.
- NELSON, J. B. & RILEY, D. P. (1945). *Proc. Phys. Soc.* **57**, 160–177.
- ONUKI, Y., SHIBUTANI, K., HIRAI, T., KOMATSUBARA, T., SUMIYAMA, A., ODA, Y., NAGANO, H., SATO, H. & YONEMITSU, K. (1985). *J. Phys. Soc. Jpn.* **54**, 2804–2807.
- ONUKI, Y., SHIBUTANI, K., YAMAZAKI, T., KOMATSUBARA, T., MAEZAWA, K. & WAKABAYASHI, S. (1987). *J. Magn. Magn. Mater.* **63/64**, 306–308.
- ROSSAT-MIGNOD, J., REGNAULT, L. P., JACOUD, J. L., VETTIER, C., LEJAY, P., FLOUQUET, J., WALKER, E., JACCARD, D. & AMATO, A. (1988). *J. Magn. Magn. Mater.* **76/77**, 376–384.
- SCHLAGER, H. G., SCHRÖDER, A., WELSCH, M. & LÖHNEYSEN, H. v. (1993). *J. Low Temp. Phys.* **90**, 181–204.
- SCHRÖDER, A., SCHLAGER, H. G. & LÖHNEYSEN, H. v. (1992). *J. Magn. Mater.* **108**, 47–48.
- SHELDRIK, G. M. (1976). *SHELX76 Program for Crystal Structure Determination*. Univ. of Cambridge, England.
- TRAPPMANN, T. (1991). Diploma thesis, Univ. of Karlsruhe, Germany.
- VILLARS, P., MATTHIS, K. & HULLIGER, F. (1989). *The Structure of Binary Compounds*, edited by F. R. DE BOER & D. G. PETTIFOR, pp. 1–103. Amsterdam: North-Holland.
- VRTIS, M. L., JORGENSEN, J. D. & HINKS, D. G. (1986). *Physica B*, **136**, 489–492.

*Acta Cryst.* (1993). **B49**, 941–951

## A Composite Modulated Structure Approach to the Lanthanide Oxide Fluoride, Uranium Nitride Fluoride and Zirconium Nitride Fluoride Solid-Solution Fields

BY R. L. WITHERS, S. SCHMID AND J. G. THOMPSON

*Research School of Chemistry, Australian National University, Canberra, ACT 0200, Australia*

(Received 22 February 1993; accepted 28 May 1993)

### Abstract

It is shown that the only generally applicable crystallographic approach to the anion excess, fluorite-related solid-solution fields reported in the zirconium nitride fluoride, uranium nitride fluoride and lanthanide oxide fluoride systems is a composite modulated structure approach. A TEM and powder XRD study has been made of the  $ZrN_xF_{4-3x}$  ( $0.906 < x < 0.936$ ) system. The appropriate superspace-group symmetries characterizing the  $Q$  and  $H$  sub-structures (and indeed the entire composite modulated structure) are shown to be  $P:Abmm:1s\bar{1}$  ( $a_Q \approx 5.2$ ,  $b_Q \approx 5.4$ ,  $c_Q \approx 5.4$  Å,  $\mathbf{q}_Q = -\mathbf{c}_Q^* + [\mathbf{c}_H^* - \mathbf{c}_Q^*]$ ) if the description used is based upon the  $Q$  sub-structure and  $B:Pmcm:s\bar{1}$  ( $a_H = a_Q \approx 5.2$ ,  $b_H = \frac{1}{2}b_Q \approx 2.7$ ,  $c_H = (p/q)c_Q$  ( $p < q$ )  $\approx 0.845c_Q \approx 4.56$  Å,  $\mathbf{q}_H = \frac{1}{2}\mathbf{b}_H^* + [\mathbf{c}_H^* - \mathbf{c}_Q^*]$ ) if the description used is based upon the  $H$  sub-structure. The relationships between the reciprocal lattices of the component sub-structures are given by  $\mathbf{a}_H^* = \mathbf{a}_Q^*$ ,  $\mathbf{b}_H^* = 2\mathbf{b}_Q^*$  and  $\mathbf{c}_H^* \approx 1.183\mathbf{c}_Q^*$ . Fourier decomposition of the previously reported conventional superstructure refinement of one member of this solid-solution field,  $Zr_{108}N_{98}F_{138}$ , has provided both underlying parent sub-structures as well as an approximation to the atomic modulation functions (AMF's) describing the mutual influence of the two parent sub-structures upon each other. In addition, such a Fourier decomposition has given an indication of the sorts of problems that will inevitably be encountered in accurately determining the appropriate AMF's when

a conventional superstructure refinement of such composite modulated structures is attempted.

### 1. Introduction

At an anion to cation ratio around 2.10–2.20 (*i.e.*  $\sim MX_{2.10}$  to  $MX_{2.20}$ ) an anion excess, fluorite-related solid-solution field, within which each and every composition has its own unique (but closely related) structure, has been reported in the zirconium nitride fluoride, uranium nitride fluoride and (a range of) lanthanide oxide fluoride systems (Abaouz, 1988; Mann & Bevan, 1972; Jung & Juza, 1973). Based upon several reported structure refinements (Bevan & Mann, 1975; Bevan, Mohyla, Hoskins & Steen, 1990; Jung & Juza, 1973) within the above solid-solution fields, Makovicky & Hyde (1981, 1992) and Hyde & Andersson (1989) described such systems as vernier or misfit-layer structures in which pseudo-tetragonal unit layers of edge-connected  $\{X\}M_4$  tetrahedra (consisting of a  $4^4$  net of anions sandwiched between similar, but lower density, nets of cations *i.e.* a  $\{100\}$  layer of fluorite type) alternate with pseudo-hexagonal  $3^6$  nets of anions (see Fig. 1). The most extensively studied of such solid-solution fields is the  $YO_xF_{3-2x}$  ( $0.78 < x < 0.87$ ) system. Phase-analysis studies of this system by Mann & Bevan (1972) showed that each and every composition within the stoichiometric range  $YX_{2.12}$  to  $YX_{2.22}$  ( $X = O, F$ ) had its own unique structure *i.e.* no diphasic regions could be detected within